UK/04-13

Study of pentaquarks on the lattice with overlap fermions

N. Mathur [a], F.X. Lee [b,c], A. Alexandru [a], C. Bennhold [b], Y. Chen [d], S.J. Dong [a], T. Draper [a], I. Horváth [a], K.F. Liu [a], S. Tamhankar [a], J.B. Zhang [e]

[a] *Department of Physics & Astronomy, University of Kentucky, Lexington, KY 40506, USA*

[b] *Center for Nuclear Studies, Department of Physics, The George Washington University, Washington, DC 20052, USA*

[c] *Jefferson Lab, 12000 Jefferson Avenue, Newport News, VA 23606, USA*

[d] *Institute of High Energy Physics, Academia Sinica, Beijing 100039, P.R. China*

[e] *CSSM and Department of Physics, University of Adelaide, SA 5005, Australia*

Abstract

We present a quenched lattice QCD calculation of spin-1/2 five-quark states with $uudd\bar{s}$ quark content for both positive and negative parities. We do not observe any bound pentaquark state in these channels for either $I = 0$ or $I = 1$. The states we found are consistent with KN scattering states which are checked to exhibit the expected volume dependence of the spectral weight. The results are based on overlap-fermion propagators on two lattices, $12^3 \times 28$ and $16^3 \times 28$, with the same lattice spacing of 0.2 fm, and pion mass as low as ~ 180 MeV.

PACS numbers: 12.38.Gc, 14.20.Gk, 11.15.Ha

I. INTRODUCTION

Since the reported discovery [1] two years ago of an exotic 5-quark resonance, named $\Theta^+(uudd\bar{s})$, with a mass of about 1540 MeV and a narrow width of less than 20 MeV, there has been a rapid growth of interest in the subject. Eleven more experiments have reported the observation of the state [2]. It also stimulated the search for other pentaquarks [3]. It should be pointed out, however, that there are also ten experiments reporting negative results [4]. One has to wait for high statistics experiments to clarify the situation in order to establish the exotic state beyond doubt.

The strangeness quantum number of Θ^+ is $S = +1$, but its isospin and spin-parity assignments are undetermined by the experiments. Based just on the valence quark content, the isospin could be 0, 1, or 2. The spin-parity could be $\frac{1}{2}^{\pm}$, $\frac{3}{2}^{\pm}$, or higher. The isospin would have to be established by discovering the other charge states, while the spin-parity assignment will have to await detailed measurements of decay angular distributions.

The experiments were inspired by the Skyrme model prediction [5], and the experimental discoveries have in turn spawned intense interest on the theoretical side, with studies ranging from chiral soliton and large N_c models [6], quark models [7], KN phase-shift analysis [8], QCD sum rules [9], and recent lattice calculations [10, 11, 12].

II. INTERPOLATING FIELDS

Unlike ordinary mesons ($q\bar{q}$) and baryons (qqq), pentaquarks do not have a unique color structure aside from being a color singlet. For a spin-1/2 pentaquark state of the type $uudd\bar{s}$, there are two decay modes with different isospin content, K^0p and K^+n. The simplest local interpolating field can be written as a color-singlet configuration of a product of color-neutral meson and baryon interpolation fields,

$$\chi_1^{\mp} = \epsilon^{abc} \left(u^{Ta} C\gamma_5 d^b\right) \left[u^c \left(\bar{s}^e \gamma_5 d^e\right) \mp \{u \leftrightarrow d\}\right], \tag{1}$$

where sum over all the color indices $\{a, b, c, e\}$ is implied. The minus sign is for isospin I=0 and plus sign for I=1 respectively. A slight variation with a different color contraction is given by

$$\chi_2^{\mp} = \epsilon^{abc} \left(u^{Ta} C\gamma_5 d^b\right) \left[u^e \left(\bar{s}^e \gamma_5 d^c\right) \mp \{u \leftrightarrow d\}\right], \tag{2}$$

where the color indices e and c are positioned differently. Both interpolation fields in Eq. (1) and Eq. (2) have been used in a lattice calculation to study the pentaquark $uudd\bar{s}$ [10]. Another possible $I = 0$ interpolation field inspired by the diquark-diquark-antiquark picture is

$$\begin{aligned}\chi_3^\Gamma &= \epsilon^{gce}\epsilon^{gfh}\epsilon^{abc}\left(u^{Ta}C\gamma_5 d^b\right)\left(u^{Tf}C\Gamma d^h\right)\Gamma C^{-1}\bar{s}^{Te} \\ &= \epsilon^{abc}\left(u^{Ta}C\gamma_5 d^b\right)\left(u^{Tc}C\Gamma d^e\right)\Gamma C^{-1}\bar{s}^{Te} \\ &\quad -\epsilon^{abc}\left(u^{Ta}C\gamma_5 d^b\right)\left(u^{Te}C\Gamma d^c\right)\Gamma C^{-1}\bar{s}^{Te}, \end{aligned} \tag{3}$$

where $\Gamma = \{\mathrm{S},\mathrm{A}\} \equiv \{1, \gamma_\mu\gamma_5\}$, and we used the antisymmetric tensor relation $\epsilon^{gce}\epsilon^{gfh} = \delta^{cf}\delta^{eh} - \delta^{ch}\delta^{ef}$ to obtain the second part of the equation. The interpolation field in Eq. (3) with $\Gamma = \mathrm{S}$ has been studied in Ref. [11] and Ref. [12].

These interpolation fields couple to states with both parities. For χ_3, as for the standard nucleon interpolation field, the positive-parity state propagates in the forward (backward) time direction in the upper (lower) Dirac components of the correlation function, while the negative-parity state propagates backward (forward) in the upper (lower) components. On the other hand, for χ_1 and χ_2, the positive-parity state propagates in the forward (backward) time direction in the lower (upper) Dirac component of the correlation function, while the negative-parity state propagates backward (forward) in the lower (upper) component. In our calculations, we use both upper and lower components to improve the statistics.

In general, since χ_1^-, χ_2^- and χ_3^Γ have the same quantum numbers (*e.g.* I = 0 and $J^P = 1/2^\pm$) they should project out the same states, albeit with different spectral weights. It is interesting to note that they can be explicitly related. Indeed, despite their apparent different color-spin structures, the KN type interpolation fields and that of the diquark-diquark-antiquark type are related by a factor of γ_5 and a Fierz re-arrangement which switches the roles of the u quark and $\bar{s}$ in Eq. (1), leading to the following expression

$$\begin{aligned}(u^{Ta}C\gamma_5 d^b)\gamma_5 u^c(\bar{s}^e\gamma_5 d^e) = \quad & \frac{1}{4}(u^{Ta}C\gamma_5 d^b)(u^{Tc}Cd^e)C^{-1}\bar{s}^{Te} \\ & +\frac{1}{4}(u^{Ta}C\gamma_5 d^b)(u^{Tc}C\gamma_\mu d^e)\gamma_\mu C^{-1}\bar{s}^{Te} \\ & -\frac{1}{8}(u^{Ta}C\gamma_5 d^b)(u^{Tc}C\sigma_{\mu\nu} d^e)\sigma_{\mu\nu} C^{-1}\bar{s}^{Te} \\ & +\frac{1}{4}(u^{Ta}C\gamma_5 d^b)(u^{Tc}C\gamma_\mu\gamma_5 d^e)\gamma_\mu\gamma_5 C^{-1}\bar{s}^{Te} \\ & +\frac{1}{4}(u^{Ta}C\gamma_5 d^b)(u^{Tc}C\gamma_5 d^e)\gamma_5 C^{-1}\bar{s}^{Te}. \end{aligned} \tag{4}$$

In this expression, a sum over dummy indices μ and ν is implied, so the right-hand-side has 16 terms. We use the γ–matrix relation $\{\gamma_\mu, \gamma_\nu\} = 2\delta_{\mu\nu}$. We see that the first term on the right hand side is just the first term in the second part of Eq. (3). A similar Fierz transform of χ_2 in Eq. (2) will lead to the second term in the second part of Eq. (3). Since γ_5 multiplication reverses parity, the extra γ_5 factor in front of the u quark on the left hand side serves to match the explicit parity of both sides. Therefore, schematically one can write,

$$\begin{aligned} &\gamma_5 \times (\text{KN interpolation field}) \\ &= \tfrac{1}{2} \times (\text{diquark-diquark-antiquark interpolation field}) \\ &\qquad + \text{other terms}, \end{aligned} \tag{5}$$

where the KN interpolation field is either χ_1 or χ_2. More precisely,

$$\gamma_5 \left(\chi_1^- - \chi_2^-\right) = \frac{1}{2}\left(\chi_3^S + \chi_3^A\right). \tag{6}$$

The fact that the KN interpolation field and the diquark-diquark-antiquark interpolation field are directly related further enhances the argument that both interpolation fields couple to the same physical spectrum with different strengths. This exercise also suggests other possibilities for the diquark-diquark-antiquark interpolation fields for pentaquarks. In view of this, it is not surprising that the ground state results using KN type interpolation fields [10] largely agree with those [11] using the diquark-diquark-antiquark type. But it is a puzzle that Ref. [12], using the same diquark-diquark-antiquark type interpolation field, produces qualitatively different results than those of Ref. [10] and [11]. Although Ref. [12] uses the overlap fermion, which has better chiral properties than the Wilson fermion adopted in Refs. [10] and [11], one would not expect a qualitative difference in these calculations between the two fermion formalisms for the pion masses larger than 440 MeV. We will compare our results with these lattice calculations later.

The correlation function is obtained by Wick-contractions of all possible quark pairs. In the case of the interpolating field in Eq. (1), it has four terms. Due to isospin symmetry in the u and d quarks, the two diagonal terms are equal, and so are the two cross terms. The zero-momentum correlation function without the upper(lower) Dirac component projection reads

$$G_{5q}(t) = \sum_{\vec{x}} \langle\, \chi(x)\, \bar{\chi}(0)\, \rangle = \sum_{\vec{x}} \langle\, \chi(x)\, \bar{\chi}(0)\, \rangle_{diag} \pm\ \langle\, \chi(x)\, \bar{\chi}(0)\, \rangle_{cross}, \tag{7}$$

where the diagonal contribution is given by,

$$\sum_{\vec{x}} \langle\, \chi(x)\, \bar{\chi}(0)\, \rangle^{\alpha\beta}_{diag} \;=\; 2 \sum_{\vec{x}} \epsilon_{abc}\epsilon_{a'b'c'} \;\times$$
$$\Big\{\, S^{aa'}_{\alpha\beta}(u) \mathrm{Tr}\left[S(d)S^{\dagger}(s)\right] \mathrm{tr}\left[\underline{S}^{bb'}(d) S^{cc'}(u)\right]$$
$$- S^{aa'}_{\alpha\beta}(u) \mathrm{tr}\left[\mathcal{P}^{bb'}(d,s,d)\underline{S}^{cc'}(u)\right]$$
$$+ \left[S^{aa'}(u)\underline{S}^{bb'}(d)S^{cc'}(u)\right]_{\alpha\beta} \mathrm{Tr}\left[S(d)S^{\dagger}(s)\right]$$
$$- \left[S^{aa'}(u)\underline{\mathcal{P}}^{bb'}(d,s,d)S^{cc'}(u)\right]_{\alpha\beta} \Big\}, \tag{8}$$

and the cross contribution is

$$\sum_{\vec{x}} \langle\, \chi(x)\, \bar{\chi}(0)\, \rangle^{\alpha\beta}_{cross} \;=\; 2 \sum_{\vec{x}} \epsilon_{abc}\epsilon_{a'b'c'} \;\times$$
$$\Big\{\, \mathcal{P}^{aa'}_{\alpha\beta}(d,s,u) \mathrm{tr}\left[\underline{S}^{bb'}(d) S^{cc'}(u)\right]$$
$$+ \left[S^{aa'}(u)\underline{S}^{bb'}(d)\mathcal{P}^{cc'}(d,s,u)\right]_{\alpha\beta}$$
$$+ \left[\mathcal{P}^{aa'}(d,s,u)\underline{S}^{bb'}(d)S^{cc'}(u)\right]_{\alpha\beta}$$
$$- \left[S^{aa'}(d)\underline{\mathcal{P}}^{bb'}(d,s,u)S^{cc'}(u)\right]_{\alpha\beta} \Big\}. \tag{9}$$

In the above expression, $S \equiv S_q(x,0)$ is the fully-interacting quark propagator, $\underline{S} \equiv (\tilde{C}S\tilde{C}^{-1})^T$ with $\tilde{C} = C\gamma_5$ and $\mathcal{P}(u,s,d) = S(u)S^{\dagger}(s)S(d)$. The trace on spin-color is denoted by 'Tr' while 'tr' represents the trace on spin only. In Eq. (7) plus sign is for isospin I = 0 and minus sign for I = 1 respectively.

III. RESULTS AND DISCUSSION

Our results below are obtained on two lattices, $12^3 \times 28$, and $16^3 \times 28$, using the Iwasaki gauge action [13] and the overlap fermion action [14]. The lattice spacing of $a = 0.200(3)$ fm was determined from f_π [19] for both lattices, so the box size is L = 2.4 fm and L = 3.2 fm, respectively. Our quenched quark propagators cover a wide range of quark masses, corresponding to pion mass from 1293(20) MeV down to 182(8) MeV. The strange quark mass is set by the ϕ meson, and corresponds to a pseudoscalar mass $m_\pi \sim 760$ MeV. In Fig. 1, we plot the nucleon and the kaon masses as a function of m_π^2. A naive linear extrapolation to the physical pion mass yields a kaon mass which is within $\sim 7\%$ of the corresponding experimental value (star symbol). The Iwasaki gauge action is an $\mathcal{O}(a^2)$ renormalization-group improved action which allows the use of relatively coarse lattices without suffering

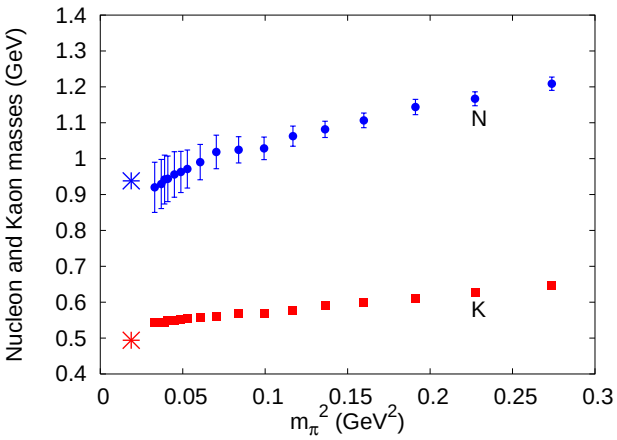

FIG. 1: Nucleon and kaon masses as a function of m_π^2 for 3.2 fm lattice. Experimental values are represented by the star symbols.

from large discretization errors. The overlap fermion action preserves exact chiral symmetry on the lattice, and thus it has no $\mathcal{O}(a)$ error. One further finds that $\mathcal{O}(a^2)$ errors are small for the meson masses [15] and renormalization constants [16, 17, 18]. Owing to the relatively gentle critical slowing down [16, 17], it allows us to work at unprecedented small quark masses. The relatively large box size ensures that the finite-volume errors are under control. At our lowest pion mass, the finite-volume error is estimated to be $\sim 2.7\%$ [19]. We have used the combination of Iwasaki gauge action and overlap fermion action with local-local correlators in a number of recent studies, including chiral logs [19] and baryon excited states [20]. To handle the excited states, we use the recently developed constrained-curve-fitting algorithm – the *sequential empirical Bayes method* [21]. The two ensembles studied here contain 80 gauge configurations each.

A. KN scattering states

It is worth noting that the entire five-quark spectrum is contained in the correlation function in Eq. (7), including a tower of KN scattering states and possible bound pentaquarks. Considering the presence of a pentaquark state, the above correlation function can be written as a sum of exponentials

$$G_{5q}(t) = W_{pen} e^{-m_{pen} t} + \sum_i W_i e^{-E^i_{KN} t} + ... \tag{10}$$

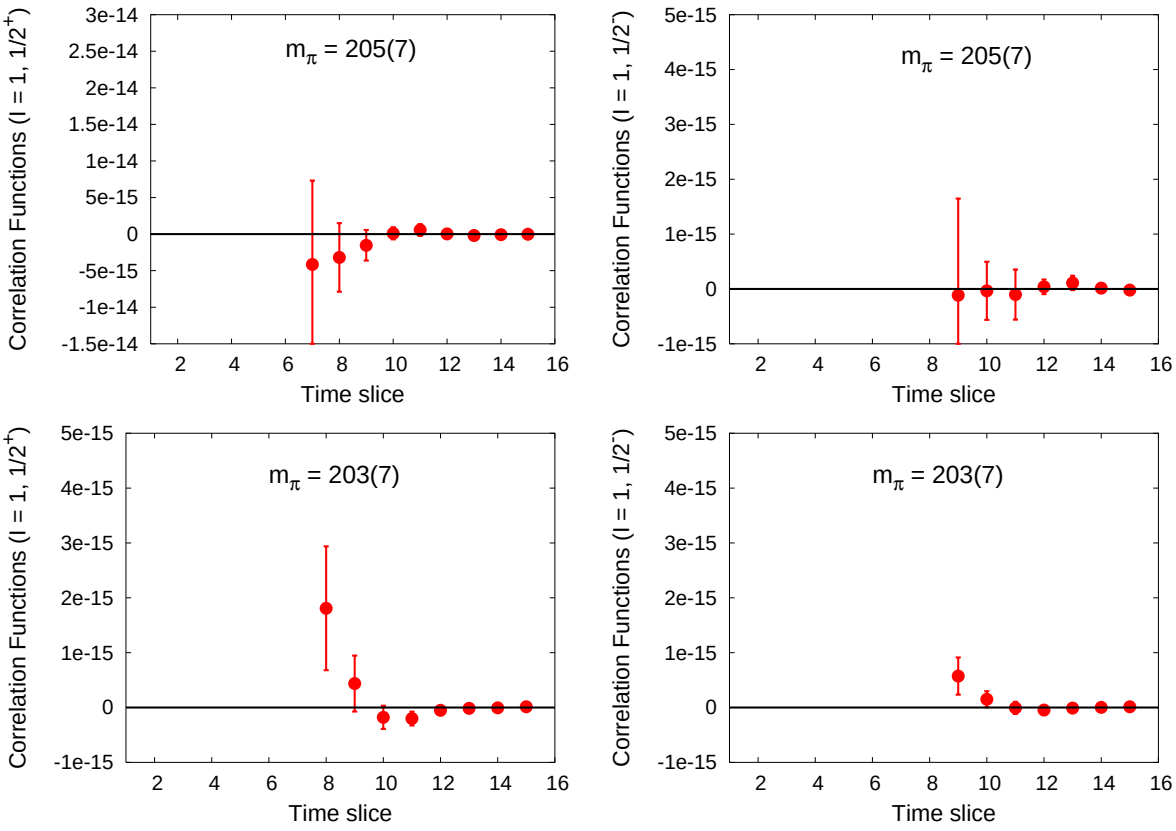

FIG. 2: Correlation functions for the positive parity (first column) and the negative parity (second column) for 2.4 fm (first row) and 3.2 fm (second row), respectively (at a pion mass around 200 MeV). One should notice that the scale in the top left figure is different than the others. This shows that for the positive parity channel the ghost state is more prominent for the smaller lattice, while no ghost state is detected for the negative parity channel.

It should be stressed that the ordering of possible pentaquark states and KN scattering states with energies E^i_{KN} in Eq. (10) is not known *a priori*, and must be determined by fitting the data. Furthermore, one needs to discern the nature of the fitted states in order to distinguish if they are KN scattering states or bound pentaquark states. The parameter E^i_{KN} denotes the KN two-particle energies with zero total momentum. Since the KN interaction is relatively weak, their values are expected to be near the two-particle threshold energy defined as

$$E_K(p) + E_N(p) = \sqrt{m_K^2 + p_K^2} + \sqrt{m_N^2 + p_N^2}. \tag{11}$$

We use the discrete momentum available on the lattice: $p_K(n) = \sqrt{n}(2/a)\sin(\pi/L)$ for the kaon and $p_N(n) = \sqrt{n}(1/a)\sin(2\pi/L)$ for the nucleon, where $n = 0, 1, 2, \cdots$. As an example,

TABLE I: The KN threshold energies corresponding to the first few discrete momenta at three different pion masses are given for the two lattices. In each block, the first column is for the $12^3 \times 28$ lattice, the second column $16^3 \times 28$ lattice.

n	E_{KN} (GeV)		E_{KN} (GeV)		E_{KN} (GeV)	
	($m_\pi = 182$ MeV)		($m_\pi = 438$ MeV)		($m_\pi = 692$ MeV)	
0	1.47	1.47	1.77	1.77	2.16	2.16
1	1.80	1.67	2.06	1.94	2.41	2.30
2	2.07	1.85	2.30	2.10	2.63	2.44
3	2.31	2.00	2.52	2.24	2.83	2.56

the KN threshold energies corresponding to the first few discrete momenta are given in Table I. On our lattice, the energies calculated from the above forms of lattice momenta deviate about 2-3% from the corresponding energies calculated from $p_K = p_N = 2\pi/L$.

We will refer to these discrete states as $p = 0$, $p = 1$ for $n = 0, n = 1$, and so on, keeping in mind that their actual values are given in Table I. One can see the expected down-shift of the states on the larger volume. The spacing between neighboring states decreases as n increases and the momentum states are somewhat more packed for heavy quark cases. The discrete KN scattering states play different roles in the positive-parity and negative-parity channels. In the positive-parity channel, they are in a relative P-wave, so the spectrum starts at $p = 1$, which has a raised threshold of 1.80 GeV at $m_\pi = 182$ MeV, while in the negative-parity channel, they are in S-wave and the spectrum starts at zero momentum with a threshold of 1.47 GeV. If there exists a pentaquark near 1.54 GeV, it would lie below (above) the KN threshold in the positive (negative) parity channel. This means that it would be much easier to extract it in the positive-parity channel than in the negative-parity channel.

The experimental values for the KN scattering length (volume) are given in Table II. The numbers are taken from Ref. [22]. The interaction is very weak in the I=0 channel (with a small attraction in the P-wave), and is slightly repulsive in the I=1 channel. The S-wave scattering length on the lattice is related to the energy shift in a finite box of length

TABLE II: Experimental values for the KN scattering length (volume).

scattering	I=0	I=1
S-wave (fm)	0.0 ± 0.03	-0.32 ± 0.02
P-wave (fm^3)	0.08 ± 0.01	-0.16 ± 0.1

L by [23]

$$E_{KN}^{\mathrm{int}} - (E_K + E_N) = -\frac{2\pi a_0}{\mu_{KN} L^3}\left[1 + c_1\frac{a_0}{L} + c_2\frac{a_0^2}{L^2}\right] + \mathcal{O}(L^{-6}), \tag{12}$$

where a_0 is the S-wave scattering length and μ_{KN} is the reduced mass of the KN system. Using the experimental numbers and neglecting c_1 and c_2, the estimated energy shift for $I = 1$ is about 8 MeV on our $16^3 \times 28$ lattice, and about 18 MeV on the $12^3 \times 28$ lattice. As it will become clear later, these values are consistent with our results. One could turn this argument around and use our simulation results to extract information on the KN scattering [24], a subject outside the focus of this work.

B. Ghost states

Since we are working in the light quark region with the quenched approximation, there is an additional complication arising from hairpin diagrams corresponding to the would-be η' meson which is degenerate in mass with the pion. The resulting states containing the would-be η' are called ghost states since they are unphysical quenched artifacts with negative spectral weights. Because of the negative weight the key signature for the presence of ghost states is the negative correlation function at very small pion mass. Such quenched artifacts have been observed in both the meson [25] and baryon [20] sectors. In the case of pentaquarks, the ghost state is $NK\eta'$ which has intrinsic positive-parity with relative S-waves among the hadrons. In the $1/2^-$ channel, there is a relative P-wave between a pair of N, K, and the ghost η'. The threshold of this state is thus raised on the lattice: for example, $E_{KN\eta'} = E_K + E_N + E_{\eta'} = \sqrt{m_K^2 + p_K^2} + m_N + \sqrt{m_\pi^2 + p_\pi^2}$ where p starts from $n = 1$ for a P-wave between K and η'. On our smaller lattice, the value is about 2.23 GeV at 188 MeV pion mass. So the ghost state in the $1/2^-$ channel lies quite high while the lowest states are expected to be the KN scattering state in S-wave threshold and the possible pentaquark.

In the $1/2^+$ channel, the situation is the opposite. The K, N, and the ghost η' are all in

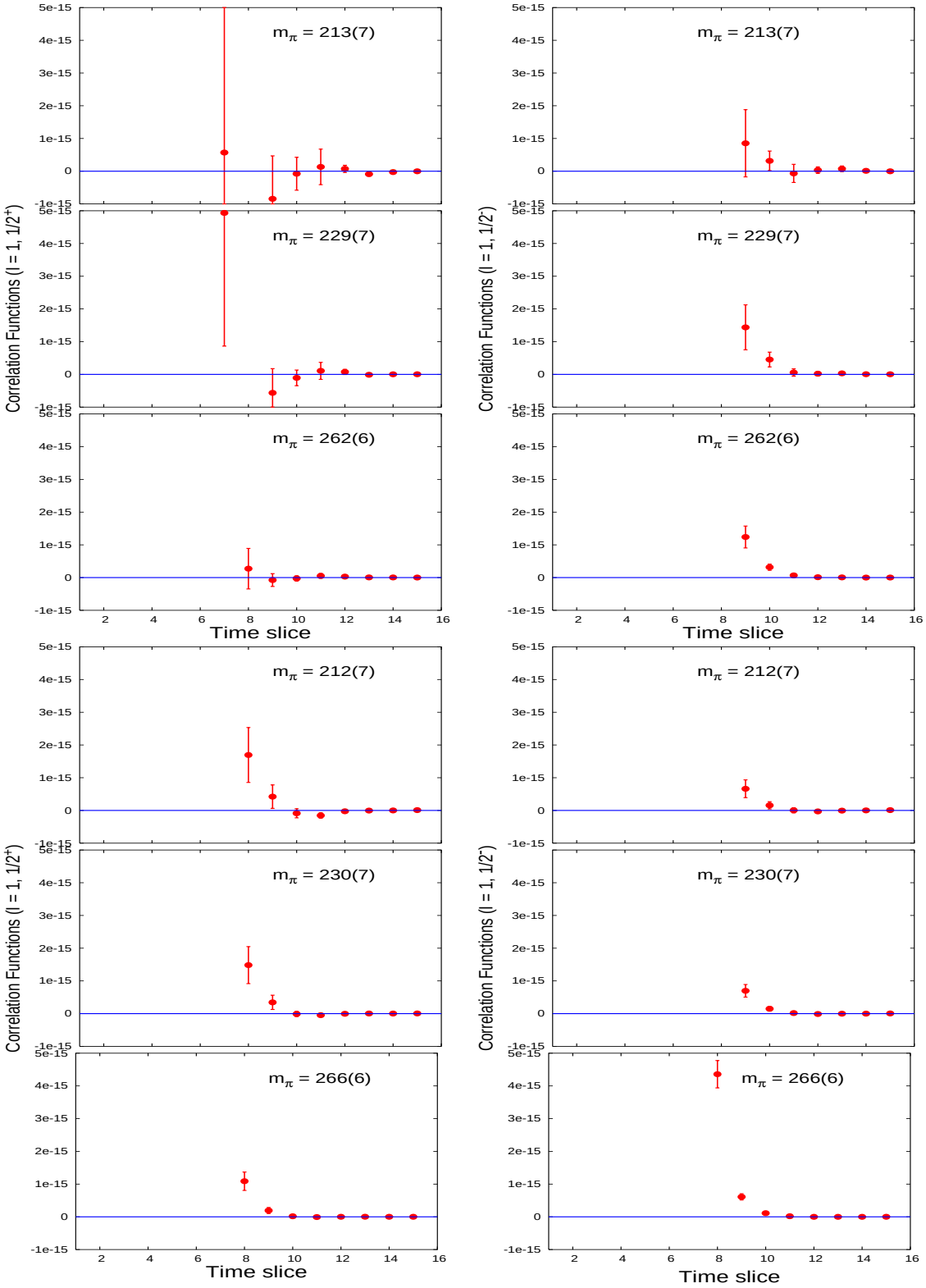

FIG. 3: Correlation functions for the positive parity (first column) and the negative parity (second column) for 2.4 fm (first three rows) and 3.2 fm (second three rows) lattices, respectively. These correlation functions are for three pion masses (in MeV). One should notice that there are negative dips in the positive parity channel which indicate the presence of ghost states. These $KN\eta'$ ghost states decouple from the correlation function at pion mass above $\sim$ 300 MeV.

relative S-wave which has a threshold of $E_{KN\eta'}(n=0) = m_K + m_N + m_\pi$. Using experimental values for pion, nucleon and kaon $E_{KN\eta'}(n=0) = 1.57$ GeV, which is right near the possible pentaquark of 1.54 GeV. So in the $1/2^+$ channel, the ghost state lies relatively low and plays a significant role, just like in the $S_{11}(1535)$ channel where the ghost state lies lower than the S_{11} when the quark mass is light [20] (i.e.with pion mass lower than 300 MeV). So in this channel, the ghost state and the potential pentaquark state are candidates for the ground state, followed by the excited state of $n = 1$ KN scattering state. In our algorithm, the ghost state is modeled as $-W_g(1 + E_\pi t)e^{-E_g t}$ where $E_\pi = \sqrt{m_\pi^2 + p_\pi^2}$ and E_g is constrained near its threshold value [20]. The fact that the ghost state has a negative spectral weight $-W_g$ is crucial for its isolation from the non-ghost states.

In Fig. 2, we present I = 1 correlation functions (at a pion mass around 200 MeV) for both parity channels and for two lattice volumes (2.4 and 3.2 fm). The top two figures are for 2.4 fm and bottom two are for 3.2 fm. A row-wise comparison of these figures reveals that the positive parity correlation functions have a negative dip which indicates the presence of quenched ghost states. On the other hand, correlation functions for the negative parity channel are always positive which confirms the absence of low-lying ghost states in that channel. Comparing the left two figures (one also has to notice the difference of scales) it is clear that the ghost states in the smaller volume are more prominent.

In Fig. 3, we plot a few more I = 1 correlation functions. As in Fig. 2, the left side figures are for positive parity and the top six figures are for the smaller volume lattice. Figures on the left side show the effect of ghost states in the correlation function. Note that the ghost states are only noticeable in the very light quark mass region. The effect of the ghost states decreases as the pion mass increases, and decouples from the correlation function near pion mass around 300 MeV. The right side figures are for the negative parity channel and they are always positive. In the previous lattice calculations [10, 11, 12], the pion masses are above 440 MeV, and therefore, there is no need to consider the ghost states. Since our lowest pion mass is 182 MeV, we will need to take the ghost states into account in the $1/2^+$ channel.

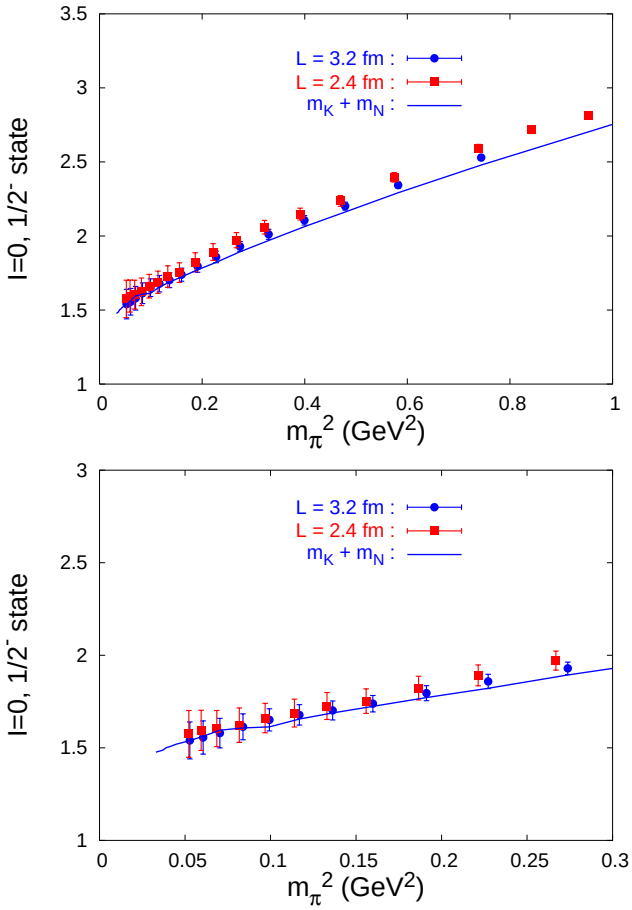

FIG. 4: The computed ground state mass in the $I(J^P) = 0\,(1/2^-)$ channel as a function of m_π^2 for the two lattices L=2.4 fm and L=3.2 fm. The curve is the KN threshold energy in the S-wave $E_{KN}(n=0) = m_K + m_N$. The bottom figure is an enlarged version of the top figure for the small quark mass region.

C. Negative-parity channel

In Figs. 4 and 5 we show the results for the ground state mass as a function of m_π^2 in the $I(J^P) = 0\,(1/2^-)$ and $1\,(1/2^-)$ channels respectively. Also plotted is the KN threshold energy in the S-wave $E_{KN}(n=0) = m_K + m_N$ which is the same on both lattices. There is no need to consider ghost states in these channels, which is supported by the fact that the correlation functions are positive throughout. The ground state energy on the smaller lattice (L=2.4 fm) is consistently higher than that on the larger one (L=3.2 fm). At the lowest mass, the energy coincides with the S-wave threshold, meaning that there is little interaction, which is consistent with the experimental fact of zero scattering length (see

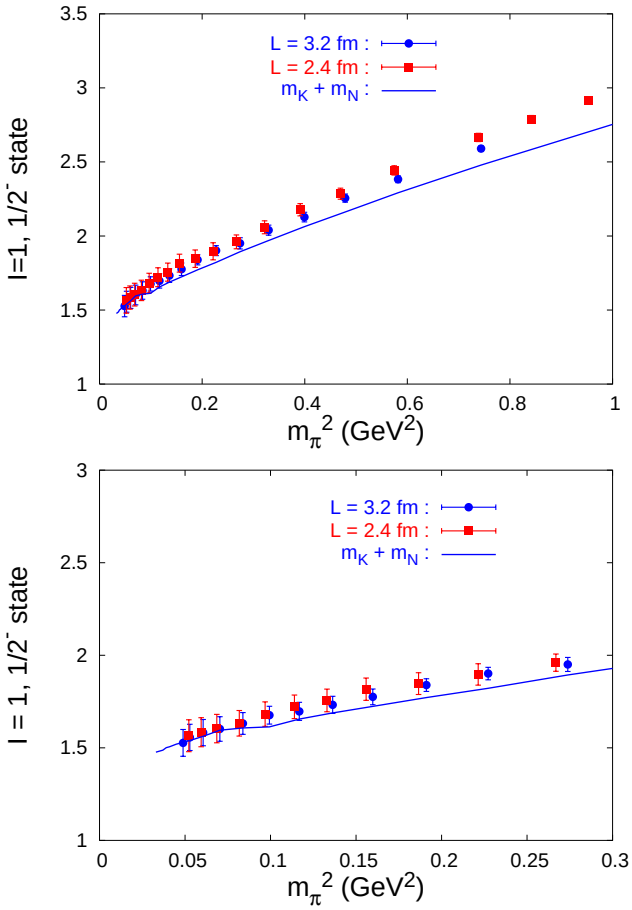

FIG. 5: The computed ground state mass in the $I(J^P) = 1\,(1/2^-)$ channel as a function of m_π^2. As above, the curve is the KN threshold energy in the S-wave $E_{KN}(n=0) = m_K + m_N$, and the bottom figure is an enlarged version of the top figure for the small quark mass region.

Table II).

Here we point out that the uncertainty in the strange mass determination (which we set by the ϕ meson and resulting in our kaon mass being higher than the experimental value by about 7%) is harmless. We note that changing the kaon mass affects both the data and the energy threshold simultaneously, so that the difference between them is essentially unaffected.

We notice that at larger m_π^2, the fitted ground state is higher than the $m_K + m_N$ threshold. In the higher quark mass region, the excited states have larger weight relative to the ground state. This, together with a somewhat smaller mass gap between different momentum states at higher quark masses, results in an effective mass which continues to drop at the largest time slices. As a result, in the higher quark mass region it is more difficult to isolate the

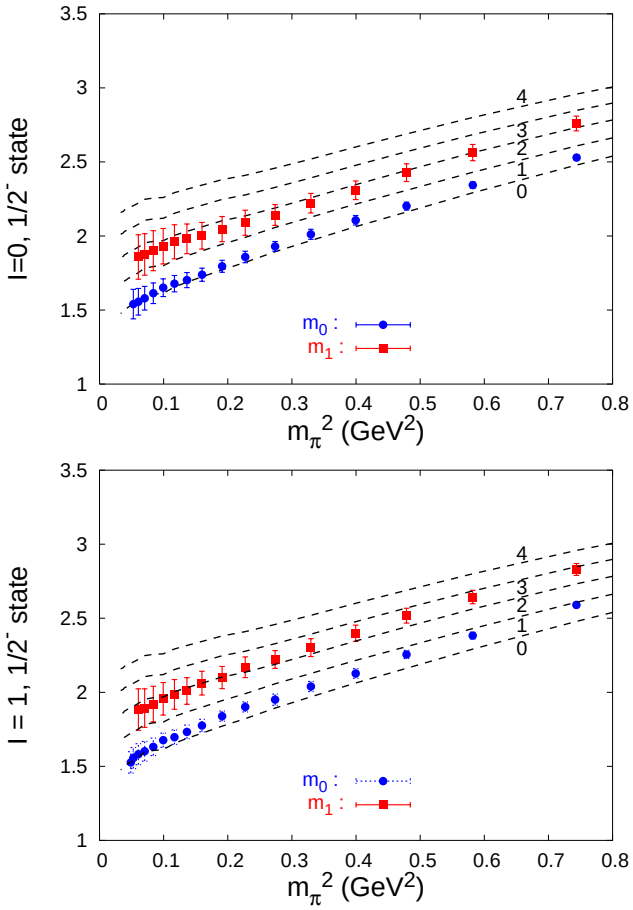

FIG. 6: The computed masses in the $I(J^P) = 0\,(1/2^-)$ (top) $1\,(1/2^-)$ (bottom) channels as a function of m_π^2 (for 3.2 fm lattice). The first excited states (square) are shown along with the ground state (circle). The first few scattering states corresponding to different discrete momenta (for n = 0,1,2,3 and 4) are shown by dashed lines.

ground state, and the fitted lowest state is a mixture of the ground state and the excited states with $n = 1$ and higher. The fact that the fitted lowest state energy on the smaller lattice (L=2.4 fm) is higher than that on the larger one (L=3.2 fm) for the same higher m_π^2 is consistent with this interpretation since the lattice momenta on the smaller lattice is larger than that on the larger lattice, leading to a mixed state with higher energy in the smaller lattice. In the low quark mass region, the excited states have smaller relative weights, and thus we are able to fit the ground state more accurately close to the mass threshold (i.e. $m_K + m_N$ with $n = 0$). However, the lack of statistics prevented us from resolving the $n = 1, 2$ and 3 states which are closely packed together [21]. As can be seen from Table I, the separation of KN states with different momenta ranges from 150 to 200 MeV which are

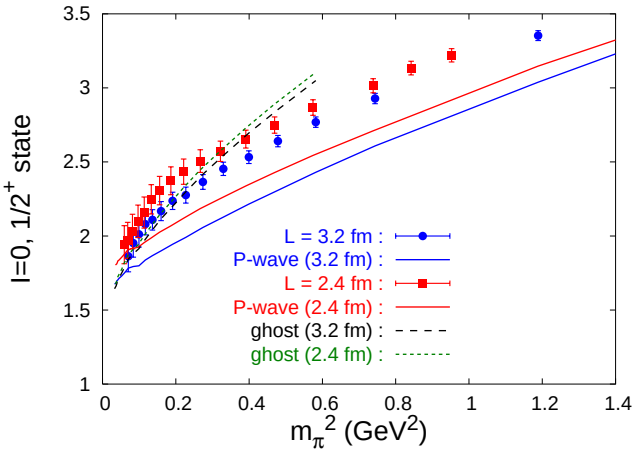

FIG. 7: The computed mass in the $I(J^P) = 0\,(1/2^+)$ channel as a function of m_π^2 for the two lattices L=2.4 fm and L=3.2 fm. The two lower curves are the KN threshold energies in the P-wave $E_{KN}(n = 1)$. The two higher curves represent the energies of the non-interacting ghost states.

much lower than the usual separation between the ground states and their radial excitations in ordinary hadrons. The latter are usually about 500 - 600 MeV. Consequently, our fitted first excited states appear to be a mixture of the $n = 1$ and higher momenta states.

As far as the ground states are concerned, our results more or less agree with those of Ref. [10] and [11], but disagree qualitatively with those of Ref. [12]. It is noted in Ref. [10] and [11] that they have seen a low-lying excited state above the KN mass threshold and they interpret it as the pentaquark state. From the top figure of Fig. 6, we see that the first excited state near the chiral limit is $\sim$ 1.85 GeV which is substantially higher than 1.54 GeV, the experimentally observed pentaquark state. As explained above, we interpret it as the mixture of the $n = 1$, $n = 2$, and possibly $n = 3$ KN scattering states. We observe similar behavior for the I = 1 case also (bottom figure). There is no candidate for a pentaquark between the KN threshold ($n = 0$) and the first KN scattering state ($n = 1$) which is contrary to the finding of Ref. [11]. We tried to accommodate an extra low-lying pentaquark state in between our ground and first excited states. However, the χ^2 fit always rejects such an intermediate state. This implies that our data do not favor a pentaquark state in between the two scattering states with lowest momenta. This, however, does not preclude a pentaquark state nearly degenerate (i.e. within 100 MeV) with the KN scattering state at threshold as was observed in Ref. [10] with a two-channel approach. We shall study

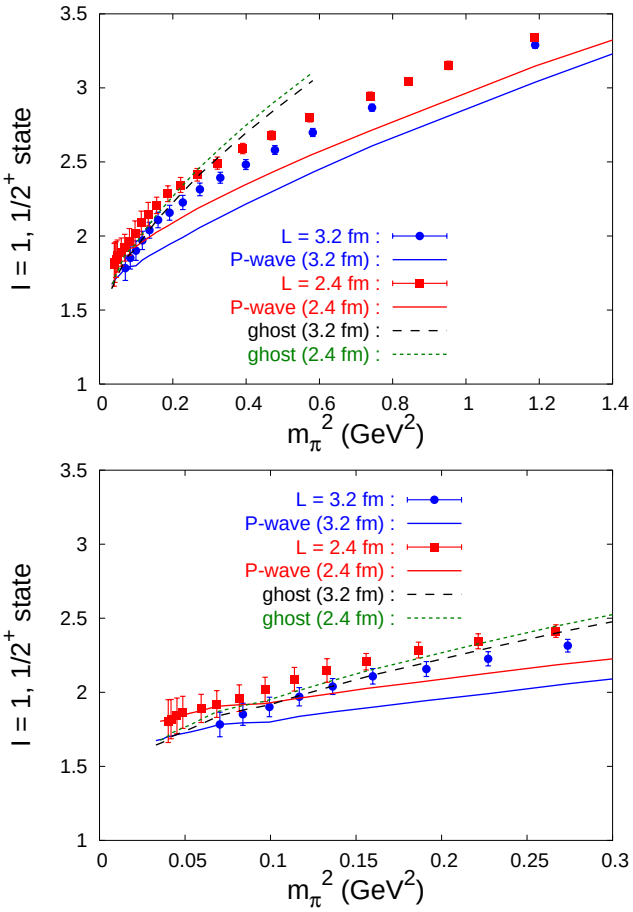

FIG. 8: The computed mass in the $I(J^P) = 1\,(1/2^+)$ channel as a function of m_π^2 for the two lattices L=2.4 fm and L=3.2 fm. The two lower curves are the KN threshold energies in the P-wave $E_{KN}(n = 1)$. The two higher curves represent the energies of the non-interacting ghost states. The bottom figure is an enlarged version of the top figure in the lower quark mass region.

this possibility in the future [26].

D. Positive-parity channel

The fitted ground state mass as a function of m_π^2 in the $I(J^P) = 0\,(1/2^+)$ and $1\,(1/2^+)$ channels are shown in Fig. 7 and Fig. 8 respectively. In these channels, the ghost $NK\eta'$ must be included, as discussed above. In the fitting model, the $NK\eta'$ ghost state, pentaquark, and KN P-wave scattering state are considered. We found a ghost state and a KN scattering state, but not a pentaquark state near 1.54 GeV. In the lower energy I = 1 channel, we have tried to see if our data could accommodate three states, but the χ^2/dof would simply reject

it. The energy of the KN scattering state lies higher on the smaller lattice (L=2.4 fm) than that on the larger lattice (L = 3.2 fm). This mainly reflects the fact that the momentum corresponding to $n = 1$ is larger on the L = 2.4 fm lattice than that of on the L = 3.2 fm lattice. At the lowest mass, the energies almost coincide with the P-wave thresholds, meaning that the KN interaction is weak, consistent with experiment. At higher m_π^2, we again observe that the ground state lies substantially higher than the P-wave KN threshold energy. We believe this is a result of a mixture with several higher momenta states, as proposed in the last section to explain the similar behavior for the negative parity states.

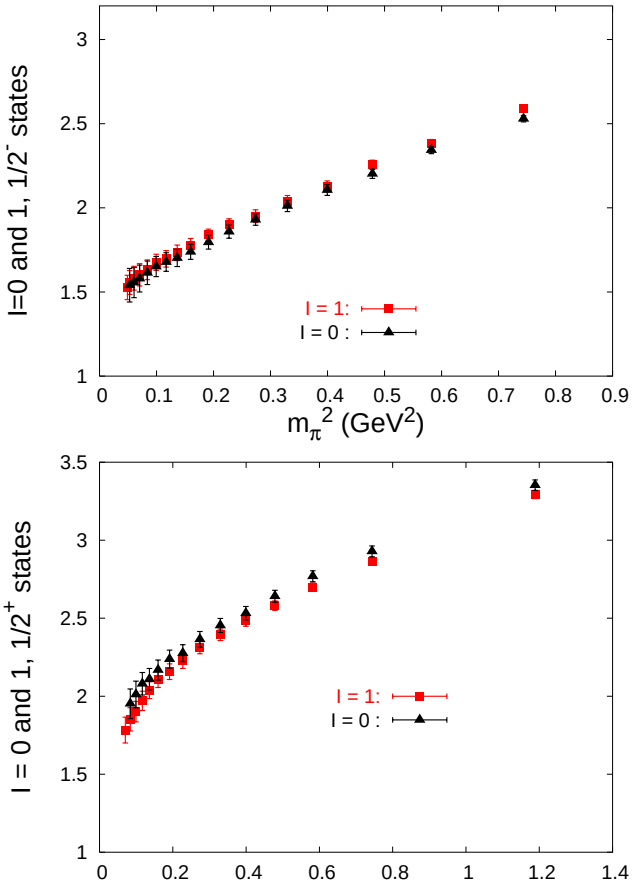

FIG. 9: A comparison of ground state masses as a function of m_π^2 for I = 0 and I = 1 channels both for the negative (top) and the positive (bottom) parities.

In Fig. 9, we compare the ground state energies for I=0 and I=1 on the 3.2 fm lattice. We observe that in the $\frac{1}{2}^-$ channel, although within errorbars, the energy of the I=1 state tends to be higher for all masses. This tendency is inverted for the $\frac{1}{2}^+$ channel. Both these observations are consistent with Ref. [10]. Our conclusion that the pentaquark state is

absent below the KN P-wave threshold again agrees with those of Ref. [10, 11] and disagrees with that of Ref. [12].

E. Volume dependence

In a box, lattice states have a volume dependence of $\sqrt{1/V}$ (where V is the spatial volume) from the normalization on the lattice. For a one-particle state, a point-source and zero momentum point-sink correlation function is given by

$$\begin{aligned} G(t) &= \sum_{\vec{x}} \langle 0|\chi(\vec{x},t)\bar{\chi}(0)|0\rangle \\ &= \sum_{n} V \frac{|\langle 0|\chi(0)|n\rangle|^2}{2M_n V} e^{-M_n t} \\ &= \sum_{n} W_n e^{-M_n t} \end{aligned} \tag{13}$$

where

$$W_n = \frac{|\langle 0|\chi(0)|n\rangle|^2}{2M_n} \tag{14}$$

is the spectral weight corresponding to the mass M_n, which has no explicit volume dependence. On the other hand, for a non-interacting two-particle scattering state, with a total zero momentum, the corresponding correlation function can be written as

$$\begin{aligned} G(t) &= \sum_{\vec{x}} \langle 0|\chi_1(\vec{x},t)\chi_2(\vec{x},t)\bar{\chi}_1(0)\bar{\chi}_2(0)|0\rangle \\ &= \sum_{n_1 n_2} V \frac{|\langle 0|\chi_1(0)|n_1\rangle|^2 |\langle 0|\chi_2(0)|n_2\rangle|^2}{2E_{n_1} V\, 2E_{n_2} V} e^{-(E_{n_1}+E_{n_2})t} \\ &= \sum_{n_1 n_2} \frac{W_{n_1} W_{n_2}}{V} e^{-(E_{n_1}+E_{n_2})t} \end{aligned} \tag{15}$$

which has an explicit inverse volume factor. Though the total momentum between the two particles is zero they can have finite lattice momentum, and thus, in Eq. 15 we used energies E_{n_1} and E_{n_2} instead of masses M_{n_1} and M_{n_2}. Since the KN interaction is very weak, approximating the spectral weight of the KN scattering state with the non-interacting expression (Eq. 15) should be a reasonable one, as far as the volume dependence is concerned. Besides the explicit volume dependence, the spectral weight in the noninteracting case i.e. $\frac{W_{n_1} W_{n_2}}{V}$ has implicit volume dependence from W_{n_1} and W_{n_2}. However, in our case, the spectral weights for the nucleon, Roper, and S_{11} have very small volume dependence (at

a few percent level) between the $12^3 \times 28$ and $16^3 \times 28$ lattices [20]. As a result, we can expect that even for a worst case the combined volume factor from W_{n_1} and W_{n_2} would be much smaller than the explicit volume factor V, which is 2.37 for our lattices. Therefore, it can be concluded that the spectral weight W for a one-particle state should not exhibit explicit volume dependence whereas a two-particle scattering state will show an explicit volume dependence in its spectral weight.

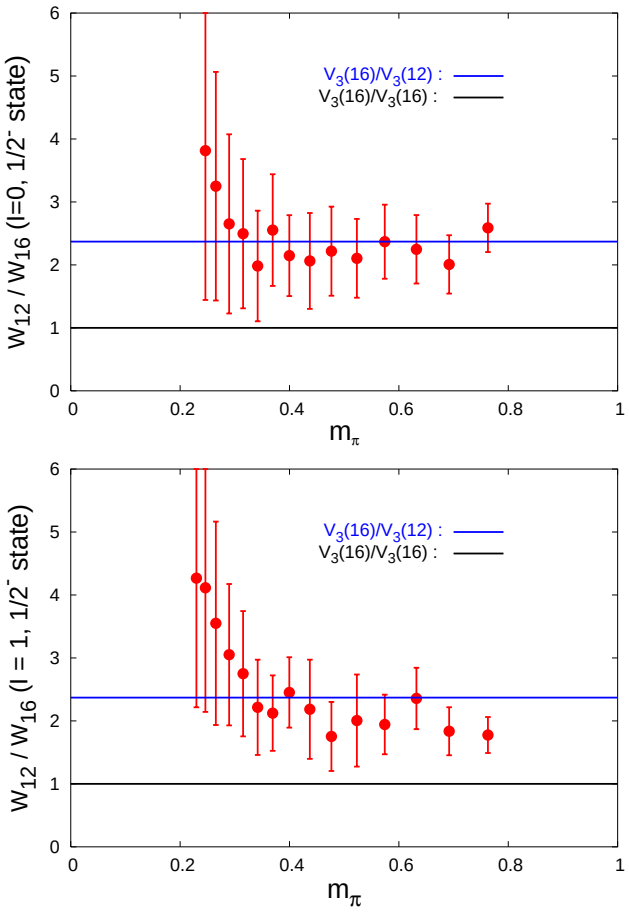

FIG. 10: Ratio of spectral weights on the two lattices in the negative parity $I = 0$ (top figure) and $I = 1$ (bottom figure) channels. The line at 2.37 is the expected volume dependence of the spectral weight.

This volume dependency of spectral weight can be exploited to check whether the state extracted is a one-particle bound pentaquark state or a two-particle KN scattering state. This is especially important to check for the negative parity channel where the threshold scattering states are close to the presumed pentaquark state. On the two lattices we used, the ratio of the spectral weights is expected to be $W(12)/W(16) \sim 16^3/12^3 = 2.37$. Fig. 10

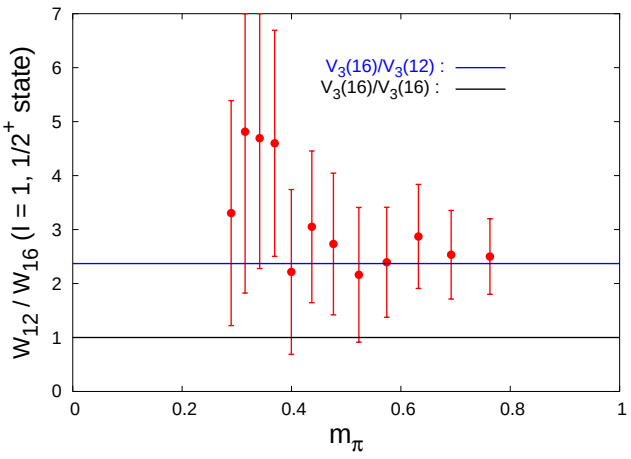

FIG. 11: Ratio of spectral weights of the two lattices for $I(J^P) = 1\,(1/2^+)$ channel. The line at 2.37 is the expected volume dependence of the spectral weight.

shows the ratio for the negative channel. Indeed it deviates significantly from unity, and the value is consistent with ~ 2.37 within error bars. This is strong supporting evidence that the observed state is a KN scattering state. The situation is similar in the positive parity channel, as shown in Fig. 11. We conclude from the volume dependence that the ground states we observe (besides the ghost states) are the KN scattering states, not the pentaquark states. Similar volume studies have been carried out earlier [20] to verify that the Roper and S_{11} states and the ghost $N\eta'$ states do have the expected one-particle and two-particle volume dependences respectively. Therefore, we caution that before concluding that a state near the KN scattering threshold is a pentaquark state, one must study the volume dependence of its spectral weight. If the weight has a large volume dependence one should not mistakenly identify it as the physical pentaquark state. The presence of KN scattering states complicates the study of possible pentaquarks in the 5-quark spectrum. It is therefore desirable to have a correlation function which is completely dominated by the two-particle scattering states and compare it with the point-source and point-sink correlators which have both the two-particle scattering states and the possible one-particle pentaquark state. One can also project out the ground state and excited state explicitly by using multi-operator cross correlators (similar to Ref. [10]). The details of such analysis will be presented elsewhere [26].

IV. CONCLUSION

Our results based on the overlap fermion with pion mass as low as $\sim$ 180 MeV seem to reveal no evidence for a pentaquark state of the type $uudd\bar{s}$ with the quantum numbers $I(J^P) = (0,1)(\frac{1}{2}^{\pm})$ near a mass of 1540 MeV. Instead, the correlation functions are dominated by KN scattering states and the ghost $KN\eta'$ states in the $1/2^+$ channel at low quark mass (pion mass less than 300 MeV). Our results are consistent with the known features of the KN scattering phase-shifts analysis [22]. We have checked that the observed KN states exhibit the expected volume dependence in the spectral weight for two particles in a box. We advocate the use of this volume dependence to uncover the character of the states found in multi-quark calculations on the lattice.

Our conclusion is in contradiction with the other lattice calculations which have claimed a pentaquark signal of either negative parity [10, 11], or positive parity [12], in the vicinity of 1.54 GeV.

Acknowledgments

We thank S. Sasaki for useful discussions. This work is supported in part by U.S. Department of Energy under grants DE-FG05-84ER40154 and DE-FG02-95ER40907. The computing resources at NERSC (operated by DOE under DE-AC03-76SF00098) are also acknowledged.

---

[1] T. Nakano *et al.* (LEPS Collaboration), Phys. Rev. Lett. **91**, 012002(2003).

[2] S. Stepanyan *et al.*, (CLAS Collaboration), Phys. Rev. Lett. **91**, 252001 (2003), hep-ex/0307018; V. Kubarovsky *et al.*, (CLAS Collaboration), Phys. Rev. Lett. **92**, 032001 (2004); V.V. Barmin *et al.* (DIANA Collaboration), Phys. Atom. Nucl. **66**, 1715 (2003), hep-ex/0304040; J.Barth *et al.* (SAPHIR Collaboration), Phys. Lett. B **572**, 127 (2003), hep-ex/0307083; A. Airapetian *et al.* (HERMES Collaboration), Phys. Lett. B **585**, 213 (2003), hep-ex/0312044; A.E.Asratyan *et al.* (neutrino), Phys. Atom. Nucl. **67**, 682 (2004), hep-ex/0309042; M. Abdel-Bary *et al.* (COSY-TOF), hep-ex/0403011 (2004); S. Chekanov *et al.*, (ZEUS Collaboration), Phys. Lett. B **591**, 7 (2004), hep-ex/0403051; A. Aleev *et al.*,

SVD collaboration, hep-ex/0401024 (2004); Yu. A. Troyan *et al.*, JINR H_2 bubble chamber, hep-ex/0404003 (2004); P.Zh. Aslanyan, *et al.*, hep-ex/0403044 (2004).

[3] NA49 Collaboration, Phys. Rev. Lett. **92**, 042003 (2004), and its critique H.G.Fischer, S.Wenig, hep-ex/0401014; H1 Collaboration, hep-ex/0403017.

[4] J.Z. Bai *et al.*, (BES Collaboration), hep-ex/0402012; K.T. Knoepfle *et al.*, (HERA-B Collaboration), hep-ex/0403020; C. Pinkenburg *et al.*, (PHENIX Collaboration), hep-ex/0404001; G. Lafferty *et al.*, OPAL Collaboration, http://www.hep.man.ac.uk/u/gdl/xmas.ppt; T. Wengler *et al.*, DELPHI Collaboration, XXXIXth Rencontres de Moriond, March 28−April 4, 2004, http://moriond.in2p3.fr/QCD/2004/Indext.html; P. Hansen *et al.*, ALEPH Collaboration, XII International Workshop on Deep Inelastic Scattering, Pleso, April 14−18, 2004, http://www.saske.sk/dis04/; D. Christian *et al.*, E690 Collaboration, QNP 2004, Bloomington, Indiana, May 23-28, 2004, http://www.qnp2004.org/; Ming-Jer Wang *et al.*, CDF Collaboration, QNP 2004, Bloomington, Indiana, May 23−28, 2004, http://www.qnp2004.org/; M.J. Longo *et al.*, HyperCP Collaboration,QNP 2004, Bloomington, Indiana, May 23−28, 2004, http://www.qnp2004.org/; J. Coleman *et al.*, BARBAR Collaboration, talk presented at the APS April meeting, http://www.slac.stanford.edu/BFROOT/.

[5] D. Diakonov, V. Petrov and M.V. Polyakov, Z. Phys. A **359**, 305 (1997);

[6] D. Diakonov, V. Petrov, hep-ph/0309203; T. Cohen, hep-ph/0309111; T. Cohen and R. Lebed, hep-ph/0309150; N. Itzhaki, I. Klebanov, P. Ouyang, L. Rastelli, Nucl. Phs. **B684**,264 (2004).

[7] R. Jaffe and F. Wilczek, Phys. Rev. Lett. **91**, 232003 (2003), hep-ph/0307341; Fl. Stancu and D.O. Riska, hep-ph/0307010; L.Y. Glozman, hep-ph/0308232; S. Capstick, P.R. Page, W. Roberts, hep-ph/0307019; C.E. Carlson, C.D. Carone, H.J. Kwee, V. Nazaryan, hep-ph/0307396.

[8] R.A. Arndt, I.I. Strakovsky, R.L. Workman, Phys. Rev. **C68**, 042201 (2003), nucl-th/0308012; R.A. Arndt, Ya.I. Azimov, M.V. Polyakov, I.I. Strakovsky, R.L. Workman, Phys. Rev. **C69**, 035208 (2004); R.L. Workman, R.A. Arndt, I.I. Strakovsky, D.M. Manley, J. Tulpan, nucl-th/0404061; B.K. Jennings, K. Maltman, hep-ph/0308286.

[9] S.L. Zhu, Phys. Rev. Lett. **91**, 232002 (2003), hep-ph/0307345; P.Z. Huang, W.Z. Deng, X.L. Chen, S.L. Zhu, Phys. Rev. **D69**, 074004 (2004), hep-ph/0311108; J. Sugiyama, T. Doi, M. Oka, hep-ph/0309271; M. Eidemuller, hep-ph/0404126; H. Kim, S.H. Lee, Y. Oh, hep-ph/0404170; R.D. Matheus, F.S. Navarra, M. Nielsen, R. Rodrigues da Silva and S.H.

Lee, Phys.Lett. **B578**, 323 (2004).

[10] F. Csikor, Z. Fodor, S.D. Katz and T.G. Kovács, JHEP **0311**, 070 (2003).

[11] S. Sasaki, hep-lat/0310014.

[12] T.W. Chiu and T.H. Hsieh, hep-ph/0403020 and hep-ph/0404007.

[13] Y. Iwasaki, Nucl. Phys. **B 258**, 141 (1985).

[14] H. Neuberger, Phys. Lett. **B 417**, 141 (1998).

[15] S.J. Dong, F.X. Lee, K.F. Liu, and J.B. Zhang, Phys. Rev. Lett. **85**, 5051 (2000).

[16] S.J. Dong, T. Draper, I. Horváth, F.X. Lee, K.F. Liu, and J.B. Zhang, Phys. Rev. D65, 054507 (2002).

[17] K.F. Liu, hep-lat/0206002.

[18] J. B. Zhang, D. B. Leinweber, K. F. Liu, A. G. Williams, hep-lat/0311030.

[19] Y. Chen, S.J. Dong, T. Draper, I. Horváth, F.X. Lee, K.F. Liu, N. Mathur, J.B. Zhang, Phys. Rev. D (in print), hep-lat/0304005.

[20] N. Mathur, Y. Chen, S.J. Dong, T. Draper, I. Horváth, F.X. Lee, K.F. Liu and J.B. Zhang, hep-ph/0306199.

[21] Y. Chen, S.J. Dong, T. Draper, I. Horváth, F.X. Lee, K.F. Liu, N. Mathur, C. Srinivasan, S. Tamhankar, J.B. Zhang, hep-lat/0405001.

[22] J.S. Hyslop, R.A. Arndt, L.D. Roper, and R.L. Workman, Phys. Rev. D **46**, 961 (1992).

[23] M. Lüscher, *Commun. Math. Phys.*, 105: 153-188, 1986.

[24] G. Meng, C Miao, X. Du and C. Liu, hep-lat/0309048.

[25] W. Bardeen, A. Duncan, E. Eichten, N. Isgur, H. Thacker, Phys. Rev. **D65**, 014509 (2002).

[26] N. Mathur *et al.*, in preparation.